

Flexible N,N,N-chelates as supports for iron and cobalt chloride complexes; synthesis, structures, DFT calculations and ethylene oligomerisation studies

Richard Cowdell,^a Christopher J. Davies,^a Stephen J. Hilton,^a Jean-Didier Maréchal,^{a,b} Gregory A. Solan,^{*a} Owen Thomas^a and John Fawcett^a

^a Department of Chemistry, University of Leicester, University Road, Leicester, UK LE1 7RH. E-mail: gas8@leicester.ac.uk

^b Department of Biochemistry, University of Leicester, University Road, Leicester, UK LE1 7RH. E-mail: gas8@leicester.ac.uk

Received 30th June 2004, Accepted 9th August 2004

First published as an Advance Article on the web 27th August 2004

The aryl-substituted *N*-picolylenediamine and diethylenetriamine ligands, (ArNHCH₂CH₂)₂{(2-C₅H₄N)CH₂}NH and (ArNHCH₂CH₂)₂NH (Ar = 2,6-Me₂C₆H₃, 2,4,6-Me₃C₆H₂), have been prepared by employing palladium-catalysed N–C(aryl) coupling reactions of the corresponding primary amines with aryl bromide. Treatment of MCl₂ with (ArNHCH₂CH₂)₂{(2-C₅H₄N)CH₂}NH affords [(ArNHCH₂CH₂)₂{(2-C₅H₄N)CH₂}NH]MCl₂ (Ar = 2,6-Me₂C₆H₃ **1a**; 2,4,6-Me₃C₆H₂ **1b**) and [(ArNHCH₂CH₂)₂{(2-C₅H₄N)CH₂}NH]FeCl₂_n (*n* = 1, Ar = 2,6-Me₂C₆H₃ **2a**; *n* = 2, 2,4,6-Me₃C₆H₂ **2b**) in high yield. The X-ray structures of **1a** and **1b** are isostructural and reveal the metal centres to adopt distorted trigonal bipyramidal geometries with the N,N,N-chelates adopting *fac*-structures. A facial coordination mode of the ligand is also observed in bimetallic **2b**, however, in **2a** the N,N,N-chelate adopts a *mer*-configuration with the metal centre adopting a geometry best described as square pyramidal. Solution studies indicate that *mer*–*fac* isomerisation is a facile process for these systems at room temperature. Quantum mechanical calculations (DFT) have been performed on **1a** and **2a**, in which the ligands employed are identical, and show the *fac*- to be marginally more stable than the *mer*-configuration for cobalt (**1a**) while for iron (**2a**) the converse is evident. Reaction of (ArNHCH₂CH₂)₂NH with CoCl₂ gave the five-coordinate complexes [(ArNHCH₂CH₂)₂NH]CoCl₂ (Ar = 2,6-Me₂C₆H₃ **3a**, 2,4,6-Me₃C₆H₂ **3b**), in which the ligand adopts a *mer*-configuration; no reaction occurred with FeCl₂. All complexes **1**–**3** act as modest ethylene oligomerisation catalysts on activation with excess methylaluminoxane (MAO); the iron systems giving linear α -olefins while the cobalt systems give mixtures of linear and branched products.

1 Introduction

The application of tridentate nitrogen donor ligand sets as supports for transition metal-based olefin polymerisation catalysts has been the source of considerable interest in recent years. Indeed, such ligands have found prominence in both early and late transition metal catalysis. In particular, diamido-donor ligands derived from aryl-substituted dien ligands (**A**, Fig. 1) have proved compatible ligands for preparing early transition metal catalysts (e.g., Zr and Hf).¹ On the other hand, the more rigid neutral bis(arylimino)pyridine ligands have led the way for generating catalysts based on iron,^{2,3} cobalt^{2,3} and vanadium centres.⁴ In common to both the dianionic and neutral N,N,N-ligands, is the presence of N-aryl substituents which can be readily modified with regard to both their steric and electronic properties. Moreover, the nature of the aryl substitution pattern may play a key role in influencing the performance of the catalyst.

We have recently been attracted by the use of more flexible nitrogen donor ligands as potential supports for late transition metal catalysts. One candidate for the role is the dipicolylamine ligand (dpa, Fig. 1) which possess a saturated backbone but lacks steric bulk and, as a result, has a propensity for formation of catalytically undesirable complexes of the type [M(dpa)]₂²⁺ (M = Fe, Co).⁵ Herein, we report our efforts at modifying the dpa ligand architecture by replacing one of the picolyl groups with a sterically variable N-aryl-substituted ethylamine to furnish a new family of ligands termed *N*-picolylen (**B**, Fig. 1). Cobalt(II) and iron(II) chloride complexes containing **B**, and also **A**, are described as are their application as precatalysts in olefin oligomerisation.

2 Results and discussion

(a) Synthesis of the ligands

The ligands [(ArNHCH₂CH₂)₂{(2-C₅H₄N)CH₂}NH] (Ar = 2,6-Me₂C₆H₃, 2,4,6-Me₃C₆H₂) were synthesised in high yield by a palladium catalysed N–C(aryl) coupling reaction of *N*-picolylenediamine [prepared by treating 2-chloroethylamine with excess 2-(aminomethyl)pyridine] with one equivalent of the corresponding aryl bromide (Scheme 1) using experimental protocols established by Buchwald and Hartwig.⁶ A similar palladium catalysed coupling reaction was employed for the synthesis of [(ArNHCH₂CH₂)₂NH] (Ar = 2,6-Me₂C₆H₃, 2,4,6-Me₃C₆H₂)^{1b} by treating diethylenetriamine with either two equivalents of 2-bromo-*m*-xylene or 2-bromomesitylene, respectively. All the new ligands have been characterised by IR, ¹H and ¹³C NMR spectroscopy, mass spectrometry (FAB or ES) (see Experimental section).

(b) Synthesis of the complexes

(i) Reaction of MCl₂ with (ArNHCH₂CH₂)₂{(2-C₅H₄N)CH₂}NH. The reaction of (ArNHCH₂CH₂)₂{(2-

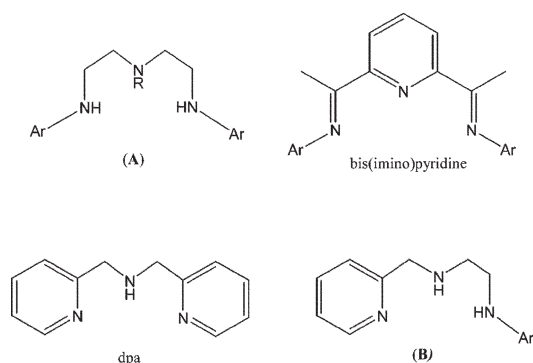
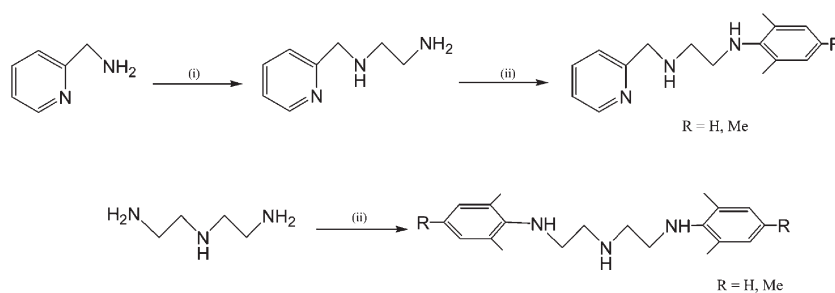


Fig. 1 Aryl-substituted dien (**A**), bis(imino)pyridine, dpa and *N*-picolylen (**B**) ligands.



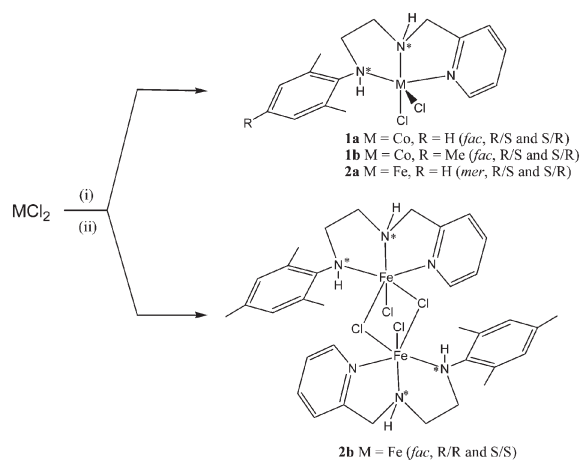
Scheme 1 Reagents and conditions: (i) NaOH, $\text{H}_2\text{NCH}_2\text{CH}_2\text{Cl}\cdot\text{HCl}$, EtOH, heat, 2 h; (ii) Ar-Br (Ar = 2,6-Me₂C₆H₃, 2,4,6-Me₃C₆H₂), NaOBu^t, Pd₂(dba)₃, *rac*-BINAP, toluene, heat, 4 days.

Table 1 Spectroscopic and analytical data for the new complexes 1–3

Compound	$\mu_{\text{eff}}^a/\mu_{\text{B}}$	$\nu(\text{N-H})^b/\text{cm}^{-1}$	FAB mass spectrum	Microanalysis (%) ^c		
				C	H	N
1a	3.8	3213w	385 (M^+), 350 ($M^+ - \text{Cl}$), 314 ($M^+ - 2\text{Cl}$)	50.01 (49.87)	5.61 (5.45)	10.80 (10.91)
1b	3.7	3136w	399 (M^+), 364 ($M^+ - \text{Cl}$), 328 ($M^+ - 2\text{Cl}$)	51.84 (51.80)	5.97 (5.90)	12.61 (12.70)
2a	4.9	3171w	755 ($2M^+ - \text{Cl}$), 347 ($M^+ - \text{Cl}$), 311 ($M^+ - 2\text{Cl}$)	49.65 (50.26)	5.62 (5.50)	10.62 (10.99)
2b	7.4	3125w	755 ($M^+ - \text{Cl}$), 395 ($M^+/2$), 361 ($M^+/2 - \text{Cl}$),	51.59 (51.52)	5.51 (5.81)	10.70 (10.61)
3a	3.9	3156w	441 (M^+), 405 ($M^+ - \text{Cl}$), 370 ($M^+ - 2\text{Cl}$)	54.07 (54.42)	6.53 (6.58)	9.15 (9.52)
3b	4.0	3335w	469 (M^+), 434 ($M^+ - \text{Cl}$), 398 ($M^+ - 2\text{Cl}$)	56.11 (56.29)	6.99 (7.04)	8.67 (8.96)

^a Recorded on an Evans Balance at room temperature. ^b Recorded on a Perkin-Elmer Spectrum One FT-IR spectrometer on solid samples. ^c Calculated values are shown in parentheses.

$\text{C}_5\text{H}_4\text{N}\text{CH}_2\text{NH}$ with MCl_2 (M = Co, Fe) in *n*-BuOH at elevated temperature gave complexes $[\{(\text{ArNHCH}_2\text{CH}_2)\{(2\text{-C}_5\text{H}_4\text{N})\text{CH}_2\text{NH}\}\text{CoCl}_2]$ (Ar = 2,6-Me₂C₆H₃ **1a**, 2,4,6-Me₃C₆H₂ **1b**) and $[\{(\text{ArNHCH}_2\text{CH}_2)\{(2\text{-C}_5\text{H}_4\text{N})\text{CH}_2\text{NH}\}\text{FeCl}_2\}_n]$ ($n = 1$, Ar = 2,6-Me₂C₆H₃ **2a**; $n = 2$, Ar = 2,4,6-Me₃C₆H₂ **2b**) in high yield (Scheme 2). All products have been characterised by FAB mass spectrometry, magnetic susceptibility, IR spectroscopy and by elemental analysis (see Table 1). In addition, crystals of **1a**, **1b**, **2a** and **2b** have been subject to single crystal X-ray diffraction studies.



Scheme 2 Reagents and conditions: (i) *n*-BuOH, 90 °C; (ii) $(\text{ArNHCH}_2\text{CH}_2)\{(2\text{-C}_5\text{H}_4\text{N})\text{CH}_2\text{NH}\}$ (Ar = 2,6-Me₂C₆H₃, 2,4,6-Me₃C₆H₂), *n*-BuOH, 90 °C; * refers to the site of chiral centre.

Dark blue single crystals of **1a** and **1b** suitable for the X-ray determination were grown by layering an acetonitrile solution of the corresponding complex with hexane at ambient temperature. The structures of **1a** and **1b** are essentially the same and only **1b** will be discussed in detail. A view of **1b** is shown in Fig. 2; selected bond distances and angles are listed for both **1a** and **1b** in Table 2. The structure of **1b** comprises a single cobalt atom surrounded by a mesityl-substituted *N*-picolythylenediamine ligand and two monodentate chloride ligands. The geometry at cobalt can be best described as distorted trigonal bipyramidal with N(2) and Cl(2) defining the axial sites [N(2)–Co(1)–Cl(2) 171.10(5)°] and N(1), Cl(1) and N(3) the equatorial sites

[N(1)–Co(1)–N(3) 109.78(6)°, N(1)–Co(1)–Cl(1) 107.97(5)°, N(3)–Co(1)–Cl(2) 95.27(5)°]. The N,N,N-chelate adopts a *fac* configuration with N(1) located 1.871(1) Å out of the plane defined by N(3)–N(2)–Co(1). The aryl group is oriented such that the *ortho*-methyl groups [C(15), C(16)] are positioned above and the below the plane defined by N(3)–N(2)–Co(1) [torsion angle: C(10)–C(9)–N(3)–Co(1) 46.4(1)°] with one *ortho*-methyl [C(15)] pointing in a similar direction to the equatorial chloride atom [Cl(1)]. The Co–N distances are far from equivalent with the longest involving the aryl-substituted amine nitrogen [Co(1)–N(3) 2.209(1) Å] and the shortest involving the pyridyl nitrogen [Co(1)–N(1) 2.089(2) Å]; the shortness of the latter can presumably be attributed to some $d\pi\text{-}p\pi$ overlap between metals and pyridyl nitrogen atoms. There is also a difference observed for the Co–Cl distances with the equatorial chloride being longer than the axial chloride [Co(1)–Cl(1) 2.360(1) Å vs. Co(1)–Cl(2) 2.283(1) Å]. The Cl–Co–Cl angle at 103.09(2)° falls below the range found in bis(imino)pyridine-containing cobalt dichloride complexes⁷ but compares well with less rigid N,N,N-chelated five-coordinate cobalt dichloride complexes.⁸ Due to the centric nature of the space group, both *R/R* and *S/S* forms are present for the two chiral centres at N(1) and N(2) in the crystal of **1b** (also **1a**).

In the FAB mass spectrum of **1a** and **1b** molecular ion peaks are observed along with fragmentation peaks corresponding to the loss of chloride ligands; very minor peaks relating to dimeric species are also evident. In the IR spectrum the $\nu(\text{N-H})$ absorption bands are seen at *ca.* 3175 cm⁻¹ and shifted to a lower wavenumber than that in the corresponding free ligands. The magnetic susceptibility measurements for **1a** and **1b** reveal magnetic moments of *ca.* 3.75 μ_{B} (Evans balance at ambient temperature) which are consistent with high spin configurations possessing three unpaired electrons.

Golden coloured crystals of **2a** and **2b** suitable for the X-ray determination were grown by layering an acetonitrile solution of the corresponding complex with hexane at room temperature. The structures of **2a** and **2b** are dissimilar and will be discussed separately. The molecular structure of **2a** is illustrated in Fig. 3; selected bond distances and angles are listed in Table 2.

The structure of **2a** is based on an iron atom bound by a 2,6-dimethylphenyl-substituted *N*-picolythylenediamine ligand and two monodentate chloride ligands. The geometry at iron is distorted square pyramidal with N(1), N(2), N(3) and Cl(2)

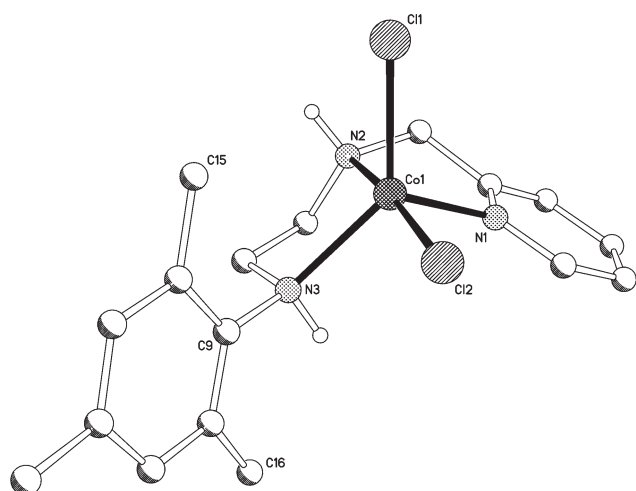


Fig. 2 Molecular structure of **1b** including the atom numbering scheme. All hydrogen atoms except for H2 and H3 have been omitted for clarity.

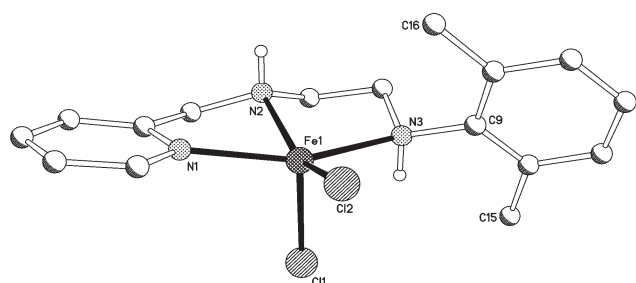


Fig. 3 Molecular structure of **2a** including the atom numbering scheme. All hydrogen atoms except for H2 and H3 have been omitted for clarity.

defining the square base and Cl(1) the apex. The N,N,N-chelate adopts a *mer*-configuration with the N(1)–Fe(1)–N(3) angle being 153.28(6)° and the deviation from planarity displayed by the N(1)–N(2)–N(3)–Fe(1) plane minimal [max. deviation: Fe(1) 0.018 Å]. The secondary amine terminus of the ligand possesses the aryl substituent which is inclined at an angle of 69.2(1)° to the N(1)–N(2)–N(3)–Fe(1) plane with its *ipso*-carbon atom [C(9)] sitting 0.733(1) Å out of the plane and on the same side as Cl(2). The *ortho*-methyl groups of the aryl group sit above and below the N(1)–N(2)–N(3)–Fe(1) plane [deviation from plane: C(16) 2.923(1), C(15) 1.478(1) Å], with C(16) pointing in a similar direction to Cl(1). There is a difference in the Fe–N bond lengths with the distance to the pyridyl donor being the shortest [Fe(1)–N(1) 2.178(1) Å] and to the arylamine the longest [Fe(1)–N(3) 2.296(1) Å]. Similarly, the Fe–Cl distances are asymmetric with the distance to the apical chloride the longest [Fe(1)–Cl(1) 2.398(1) Å vs. Fe(1)–Cl(2) 2.285(1) Å]. The Cl–Fe–Cl angle at 109.24(2)° falls in the lower end of the range for the corresponding angle in related complexes.⁹ As with **1a** and **1b**, both *R/R* and *S/S* forms of the complex are present within the crystal of **2a**.

The molecular structure of **2b** is shown in Fig. 4; selected bond distances and angles are listed in Table 3. The structure consists of a dimeric unit generated through a crystallographically imposed inversion centre. The iron centres are bridged by two chloride ligands and bound terminally by a chloride and a mesityl-substituted *N*-picolylen ligand to give a pseudo-octahedral geometry at each metal centre. The two *N*-picolylen ligands adopt facial bonding modes such that the pyridyl and the aryl-substituted amine moieties are *trans* to the bridging chlorides and the central amine *trans* to a terminal chloride. At each metal centre the pyridyl nitrogen–iron distance [Fe(1)–N(1) 2.168(2) Å] is the shortest of the three Fe–N distances while the aryl-substituted amine–iron distance the longest [Fe(1)–N(3) 2.334(2) Å]. The Fe– μ -Cl distances are similar [Fe(1)–Cl(1) 2.509(1), Fe(1)–Cl(1A) 2.546(1) Å] and

Table 2 Selected bond distances (Å) and angles (°) for **1a**, **1b** and **2a**

	M = Co (1a)	M = Co (1b)	M = Fe (2a)
M(1)–N(1)	2.082(1)	2.089(2)	2.178(1)
M(1)–N(2)	2.188(1)	2.179(2)	2.185(1)
M(1)–N(3)	2.168(1)	2.209(2)	2.296(1)
M(1)–Cl(1)	2.347(1)	2.360(1)	2.398(1)
M(1)–Cl(2)	2.296(1)	2.283(1)	2.285(1)
Cl(1)–M(1)–N(1)	105.79(4)	107.97(5)	101.16(4)
Cl(1)–M(1)–N(2)	87.42(3)	85.78(5)	99.92(4)
Cl(1)–M(1)–N(3)	141.63(4)	134.59(5)	84.72(4)
Cl(1)–M(1)–Cl(2)	104.30(2)	103.09(2)	109.24(2)
Cl(2)–M(1)–N(1)	98.71(4)	98.69(5)	98.19(4)
Cl(2)–M(1)–N(2)	168.22(4)	171.10(5)	150.84(4)
Cl(2)–M(1)–N(3)	91.95(3)	95.27(5)	104.46(4)
N(1)–M(1)–N(3)	105.72(5)	109.78(6)	153.28(6)
N(1)–M(1)–N(2)	76.64(5)	77.49(7)	75.56(6)
N(2)–M(1)–N(3)	79.14(5)	78.72(6)	77.75(5)

fall at the top end of the range found for related complexes.¹⁰ As expected, the Fe–Cl(terminal) bond distances [Fe(1)–Cl(2) 2.310(1) Å] are shorter than those seen for the bridging chlorides but at the top end of the range observed in structurally related complexes.¹⁰ The ClFe(μ -Cl)₂FeCl motif has been found in a number of crystallographically characterised complexes with the transannular Fe...Fe separation in **2b** [3.600(1) Å] falling in the mid-range.¹⁰ Unlike in **1a**, **1b** and **2a**, the relative configuration of the chiral centres is distinct with both *R/S* and *S/R* forms adopted within the structure of **2b**.

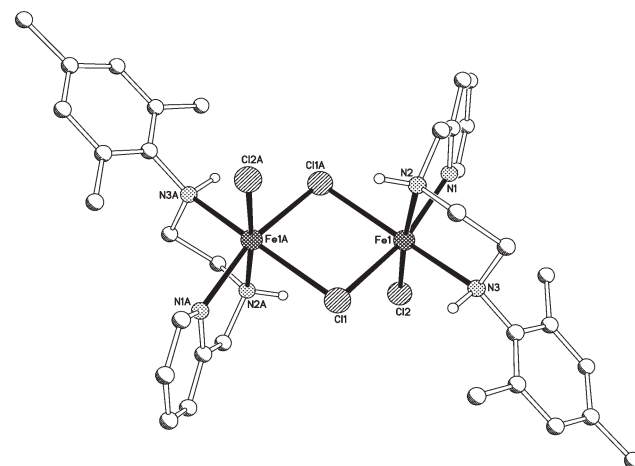


Fig. 4 Molecular structure of **2b** including the atom numbering scheme; the atoms labelled with a suffix are generated by symmetry ($-x$, $1-y$, $-z$). All hydrogen atoms except for H2 and H3 have been omitted for clarity.

Despite the molecular structures of **2a** and **2b** being monomeric and dimeric respectively, their FAB mass spectra are similar. Both show peaks consistent with the loss of a chloride ligands from a monomeric species, [(*N*-picolylen)FeCl₂], along with minor peaks attributable to chloride loss from dimeric species, [(*N*-picolylen)FeCl₂]₂. In the IR spectrum the ν (N–H) absorption bands are seen at *ca.* 3150 cm⁻¹ and shifted to a lower wavenumber than that in the corresponding free ligands. The magnetic susceptibility measurement for **2a** gives a magnetic moment of 4.9 μ_B (Evans balance at ambient temperature) which is consistent with a high spin configuration possessing four unpaired electrons. In dimeric **2b**, a magnetic moment of 7.4 μ_B is observed which is consistent with two non-interacting high spin metal centres. Indeed, cooling of **2b** down to 50 K shows little variation in the magnetic moment.¹¹

Although the complexes are paramagnetic, ¹H NMR spectroscopy can be informative. Fig. 5 shows the room temperature ¹H NMR spectra (recorded in acetonitrile-*d*₃) of monomeric **2a** and dimeric **2b**. The spectra of **2a** and **2b** show broad paramagnetically shifted peaks between –16.0 and

Table 3 Selected bond distances (Å) and angles (°) for **2b**

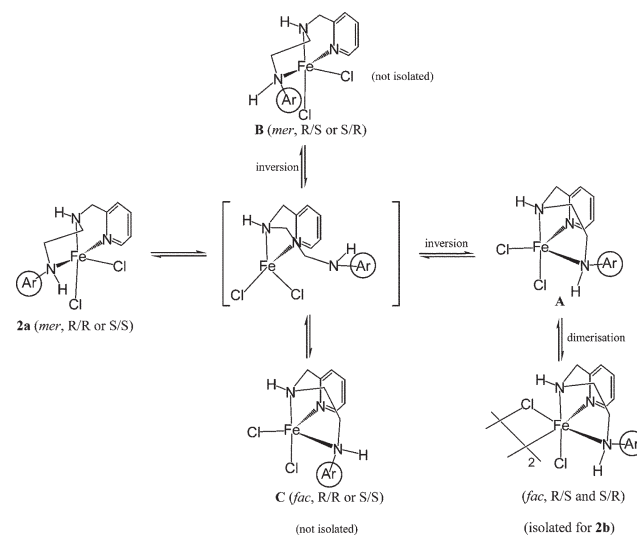
Fe(1)–N(1)	2.168(2)	Fe(1)–Cl(2)	2.310(1)
Fe(1)–N(2)	2.218(2)	Fe(1)–Cl(1A)	2.546(1)
Fe(1)–N(3)	2.334(2)	Fe(1)···Fe(1A)	3.600(1)
Fe(1)–Cl(1)	2.509(1)		
Cl(1)–Fe(1)–N(3)	81.06(6)	Cl(2)–Fe(1)–Cl(1A)	96.56(3)
Cl(1)–Fe(1)–Cl(2)	94.41(2)	N(3)–Fe(1)–N(1)	103.43(7)
Cl(1)–Fe(1)–N(1)	162.93(6)	N(3)–Fe(1)–N(2)	77.24(7)
Cl(1)–Fe(1)–Cl(1A)	89.19(2)	N(3)–Fe(1)–Cl(1A)	162.33(5)
Cl(1)–Fe(1)–N(2)	87.88(5)	N(1)–Fe(1)–N(2)	77.27(7)
Cl(2)–Fe(1)–N(1)	101.05(6)	N(1)–Fe(1)–Cl(1A)	81.94(5)
Cl(2)–Fe(1)–N(3)	98.84(5)	N(2)–Fe(1)–Cl(1A)	87.76(6)
Cl(2)–Fe(1)–N(2)	175.13(6)		

The atoms labelled with a suffix are generated by symmetry ($-x, 1-y, -z$).

131.0 ppm (Fig. 5). Some degree of assignment can be made on comparison of the chemical shifts and relaxation times in **2a** and **2b** with the related iron(II) complexes [(*fac*-dpa)FeCl(μ -Cl)₂ClFe(*fac*-dpa)] and [(tpa)FeCl₂] (tpa = tripicolylamine) in which the pyridyl (H_a , H_b and H_c) and methylene protons of the picolyl group have characteristic chemical shifts.^{5,12} Typically, H_a is observed most downfield (115–130 ppm) while H_c most upfield (6–20 ppm). In between these signals are located the H_b and CH_2 signals. The aromatic signals have been assigned on the basis of integration and by direct comparison between the two spectra (mesityl vs. 2,6-dimethylphenyl). In particular, the *para*-substituent of the aryl group can be informative with the Me_p in **2b** appearing at δ 15.7 while in **2a** this signal is absent but replaced by H_p at δ -5.4.

What is clear from the two spectra, despite the difference in the solid-state structures, both behave similarly in solution at room temperature. Scheme 3 shows a series of equilibria that can explain the apparent dynamic behaviour of **2a** and **2b**. Dissociation of the arylamino arm of the ligand in *mer*-**2a** could generate a four-coordinate iron complex containing a pendant amine group. Inversion of the stereochemistry of the pendant amine, some reorganisation of the ethyl unit, followed by recoordination would generate the *fac*-coordinated species **A**. As the bulky aryl group is now remote from the chloride ligands, dimerisation can occur to give a *fac*-coordinated dimer (isolated for **2b**). On the other hand, recoordination following inversion would generate the *mer*-species **B**, while recoordination without inversion would generate *fac*-**C**. Notably **C**, although not isolated with iron as the metal centre, has been structurally characterised for cobalt (**1a** and **1b**). Some support for the

postulated lability of the aryl-substituted arylamino arm is given on inspection of the M–N distances in **2a** and **2b**, in which the corresponding Fe–N distances are *ca.* 0.1 Å longer than the other M–N distances. A related dissociation of an amino group in a N,N,N-chelate has previously been observed in a five-coordinate group 4 system.¹³



Scheme 3 Aryl-amino nitrogen dissociation in **2a** and recoordination possibilities.

In order to probe the relative stabilities of the *mer* and *fac* isomers for the cobalt and iron chloride complexes containing aryl-substituted *N*-picolylen ligands, DFT (B3LYP) calculations were undertaken. Geometry optimisations were carried out on [((2,6-Me₂C₆H₃)NHCH₂CH₂)(2-C₅H₄N)CH₂)NH]MCl₂] [M = Co (**1a**) or Fe (**2a**)] for both *mer*-RR and *fac*-RR conformations taking into account the high spin state of all species. All unpaired electrons are located on the metal centre: four and three for the Fe and Co complexes, respectively. Different electronic repartitions of the metals d orbitals have been considered for both **1a** and **2a** and the lowest energetic ones were selected for geometry optimisation.

Optimised structures of the *fac* and *mer* complexes for **1a** and **2a** are depicted in Fig. 6; geometrical parameters are listed in Table 4. Overall, experimental and theoretical structures for *fac*-**1a** and *mer*-**2a** complexes are in good agreement. In particular, the optimised values for the internal bond lengths and angles of the tridentate ligand compare well with the experimental

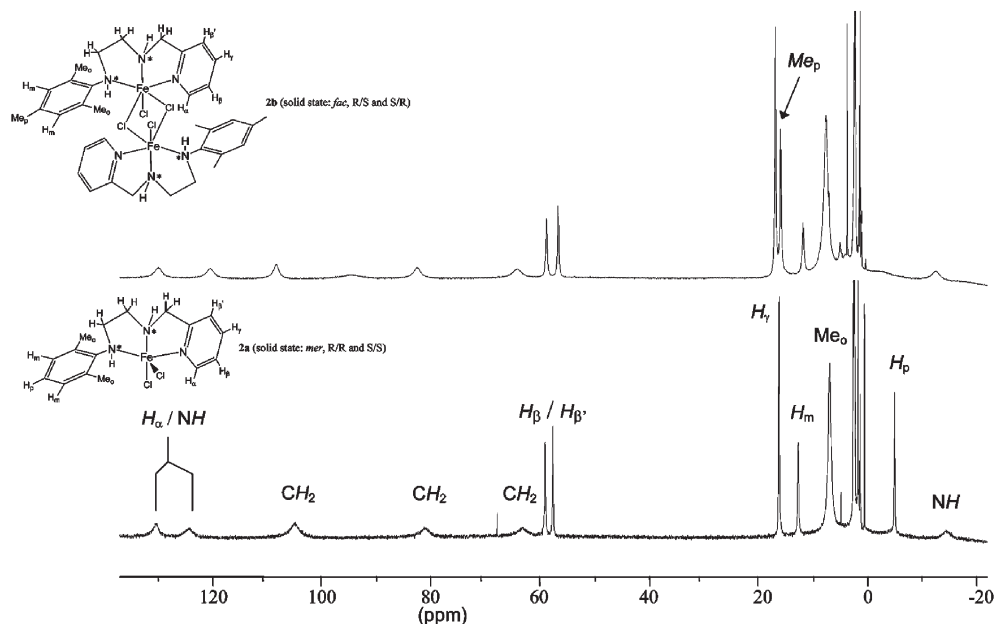


Fig. 5 Paramagnetically shifted ¹H NMR spectra for complexes **2a** and **2b** in acetonitrile-*d*₃.

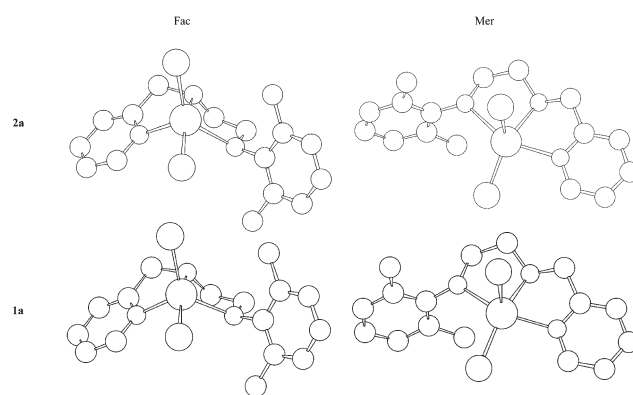
Table 4 Selected bond distances (Å) and angles (°) for *fac*-RR and *mer*-RR complexes of **1a** and **2a**

	<i>fac</i> -RR Conformers			<i>mer</i> -RR Conformers		
	Experimental M = Co (1a)	Optimised M = Co (1a)	Optimised M = Fe (2a)	Experimental M = Fe (2a)	Optimised M = Co (1a)	Optimised M = Fe (2a)
M(1)–Cl(1)	2.347	2.34	2.35	2.398	2.37	2.41
M(1)–Cl(2)	2.296	2.33	2.34	2.285	2.30	2.29
M(1)–N(1)	2.082	2.19	2.23	2.178	2.18	2.24
M(1)–N(2)	2.188	2.25	2.30	2.185	2.23	2.23
M(1)–N(3)	2.168	2.26	2.35	2.296	2.27	2.37
Cl(1)–M(1)–N(1)	105.8	108.8	106.9	101.2	104.1	95.0
Cl(1)–M(1)–N(2)	87.4	84.1	84.3	99.9	90.0	92.6
Cl(1)–M(1)–N(3)	141.6	125.4	130.9	84.7	90.3	84.6
Cl(1)–M(1)–Cl(2)	104.3	118.3	121.8	109.2	119.2	130.2
Cl(2)–M(1)–N(1)	98.7	95.0	95.7	98.2	96.3	95.4
Cl(2)–M(1)–N(2)	168.2	157.3	153.8	150.8	150.8	137.1
Cl(2)–M(1)–N(3)	91.9	90.1	86.8	104.5	102.5	106.0
N(1)–M(1)–N(2)	76.6	74.7	73.5	75.6	73.7	75.0
N(2)–M(1)–N(3)	79.1	76.4	74.8	77.7	76.7	77.2
N(1)–M(1)–N(3)	105.7	114.4	108.8	153.3	146.9	152.2

ones (values not reported). The most important discussion focused on the coordination sphere of the metal centre. The optimised M–ligand bond lengths (especially the M–N ones) are slightly longer than the experimental ones for both the *fac*-**1a** and *mer*-**2a**, with discrepancies less than 0.1 Å; discrepancies of this magnitude are sometimes observed with high spin systems studied by B3LYP.¹⁴ Further comparison of the first coordination sphere of the metal atoms reveals that some reorganisation of the ligands occurs between experimental and theoretical structures. The most noticeable is the Cl(1)–M(1)–Cl(2) angle with discrepancies of 14° in **1a** (computed 118.3° vs. experimental 104.3°) to 20.9° in **2a** (computed 130.2° vs. experimental 109.3°). Interestingly, the values of the Cl(1)–M(1)–Cl(2) optimised angles are significantly closer to those observed in the molecular structures of **3a** and **3b** (see later, 114.4 and 113.3°, respectively). To further investigate the relevance of these structural differences, geometry optimisations of *fac*-**1a** and *mer*-**2a** were carried out by fixing the Cl(1)–M(1)–Cl(2) angle to their experimental values (104.3 and 109.3° respectively), and optimising all the other geometrical variables. Comparison between experimental, fully optimised and partially optimised structures shows that the increase of the Cl(1)–M(1)–Cl(2) angle is related to the rotation of the aryl group and the pyridine (to a lesser extent) around their N–C bond. Analysis of the whole unit cell of both crystals shows that significant π -stacking and other ‘long distance’ contacts exist between monomers in the crystals. The observed rearrangements in the optimised structures are therefore associated with the vacuum condition of the calculations as compared to the packing environment of the experimental system. This observation associated with the low difference in potential energy between the partially optimised and fully optimised structures of *fac*-**1a** and *mer*-**2a** (fully optimised structures in both cases are 1.7 kcal mol⁻¹ more stable than the partially optimised ones) show that the discrepancies of the Cl(1)–M(1)–Cl(2) angle are not physically significant.

Geometry optimisations of the non-experimentally characterised structures *fac*-**2a** and *mer*-**1a** have been carried out using B3LYP and lead to two stable structures. The optimised *fac*-**2a** and *mer*-**1a** structures (Fig. 6) are in good agreement with the data presented for *fac*-**1a** and *mer*-**2a**. In particular, the bond lengths do not change significantly between the computed *fac*- and *mer*-isomers (Table 4). With regard to the Cl(1)–M(1)–Cl(2) angle, these optimised structures show the same tendency for a more accentuated angle (121.8 and 119.2° for *fac*-**2a** and *mer*-**1a** respectively) than the experimental *fac*-**2a** and *mer*-**1a** conformers. Therefore, theoretical calculations lead to two stable *fac*- and *mer*-conformers for both **1a** and **2a**.

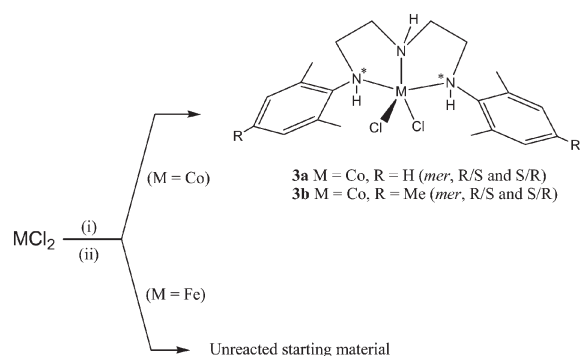
The difference in free Gibbs energy between *fac*- and *mer*-conformers for both **1a** and **2a** has been calculated with the

**Fig. 6** B3LYP optimised structures of *mer* and *fac* isomers of **1a** and **2a**.

equation $\Delta G^0 = G^0_{\text{fac}} - G^0_{\text{mer}}$. The differences of enthalpy are also provided as indicative values. For the cobalt compound **1a**, $\Delta G^0 = -1.04$ kcal mol⁻¹ ($\Delta H^0 = -0.84$ kcal mol⁻¹), and for the iron compound **2a**, $\Delta G^0 = 2.41$ kcal mol⁻¹ ($\Delta H^0 = 2.41$ kcal mol⁻¹). Several points emerge; firstly, these results show that for both cobalt and iron species, *fac*- and *mer*-conformations are very close in energy. Secondly, for **1a**, the *fac*-conformer is approximately 1 kcal mol⁻¹ more stable than the *mer* one, while for **2a**, the *mer*-conformer is approximately 2.5 kcal mol⁻¹ more stable than the *fac* one. These results concur with the experimental observations with *fac*-**1a** and *mer*-**2a** being the most stable conformers.

In summary, the computed energetics in the gas phase for the two isomers reproduce properly the nature of the most stable isomer for both cobalt and iron in the crystalline state. Indeed, the low energy difference between *fac*- and *mer*-structures for both iron and cobalt would suggest an equilibrium to be likely in solution which is confirmed by the ¹H NMR studies of **2** (*vide supra*). However, these calculations do not take into account the possible mechanism involved in the transition from one conformer to the other.

(ii) Reaction of CoCl₂ with (ArNHCH₂CH₂)₂NH. The reaction of (ArNHCH₂CH₂)₂NH with CoCl₂ in *n*-BuOH at elevated temperature gave complexes [(ArNHCH₂CH₂)₂NH]CoCl₂ (Ar = 2,6-Me₂C₆H₃ **3a**, 2,4,6-Me₃C₆H₂ **3b**) in high yield (Scheme 4). The corresponding reactions of (ArNHCH₂CH₂)₂NH with FeCl₃ gave only unreacted starting materials. All products have been characterised by FAB mass spectrometry, magnetic susceptibility and by elemental analysis (Table 1). In addition, crystals of **3a** and **3b** have been the subject of single crystal X-ray diffraction studies.



Scheme 4 Reagents and conditions: (i) *n*-BuOH, 90 °C; (ii) (ArNH-CH₂CH₂)₂NH (Ar = 2,6-Me₂C₆H₃, 2,4,6-Me₃C₆H₂), *n*-BuOH, 90 °C.

Dark blue single crystals of **3a** and **3b** suitable for the X-ray determination were grown by layering an acetonitrile solution of the corresponding complex with hexane. The structures of **3a** and **3b** are essentially the same and only **3a** will be discussed in detail. A view of **3a** is shown in Fig. 7; selected bond distances and angles are listed for both **3a** and **3b** in Table 5. The structure of **3a** consists of a cobalt atom surrounded by a single chelating tridentate 2,6-dimethylphenyl-substituted dien ligand and two monodentate chloride ligands. The five-coordinate geometry can be best described as distorted trigonal bipyramidal with N(3) and N(1) forming the axial sites and N(1), Cl(1) and Cl(2) the equatorial sites. The dien ligand adopts, unlike in **1a** and **1b**, a *mer* configuration with the N(1)–Co(1)–N(3) angle being 160.08(7)° and the deviation from planarity displayed by the N(1)–N(2)–N(3)–Co(1) plane minimal [max. deviation: Co(1) 0.063 Å]. Each terminal nitrogen atom of the dien ligand possesses an aryl substituent which are positioned mutually *cis* with both *ipso*-carbon atoms [C(11) and C(1)] *ca.* 0.68 Å below the N(1)–N(2)–N(3)–Co(1) plane and on the same side as Cl(1). The *ortho*-methyl groups of each aryl group sit above and below the N(1)–N(2)–N(3)–Co(1) plane [deviation of *o*-Me groups from plane: C(6A) 1.341(1), C(16A) 1.799(1), C(2A) 2.885(1), C(12A) 2.919(1) Å] with the two located above [C(6A) and C(16A)] pointing in a similar direction to Cl(2). There is a difference in the Co–N bond lengths with the central N–Co distance being noticeably shorter than the terminal N–Co bond lengths [Co(1)–N(2) 2.082(2) Å *vs.* Co(1)–N(1) 2.219(3), Co(1)–N(3) 2.243(2) Å]. There is also a difference observed for the Co–Cl distances with that involving Cl(2) being longer than that to Cl(1) [Co(1)–Cl(2) 2.350(1) Å *vs.* Co(1)–Cl(1) 2.269(1) Å]. The Cl–Co–Cl angle at 114.91(4)° falls in the same range as those observed for the bis(imino)pyridine-containing cobalt dichloride complexes.⁷ As with the *N*-picolylen-systems (**1** and **2**), **3** also has two chiral centres, in this case located on the termini of the N,N,N-chelate at N(1) and N(3). Both **3a** and **3b** crystallise with the relative configurations of the chiral centres being distinct.

The FAB mass spectrum of **3a** and **3b** both display molecular ion peaks and peaks corresponding to the loss of chloride ligands; no evidence for dimerised products is observed.

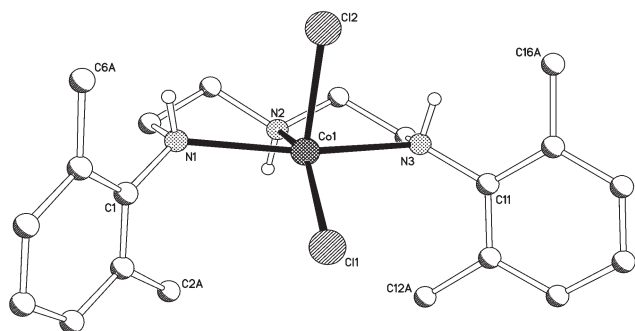


Fig. 7 Molecular structure of **3a** including the atom numbering scheme. All hydrogen atoms except for H1, H2 and H3 have been omitted for clarity.

Table 5 Selected bond distances (Å) and angles (°) for **3a** and **3b**

	3a	3b
Co(1)–N(1)	2.219(3)	2.221(4)
Co(1)–N(2)	2.082(2)	2.066(4)
Co(1)–N(3)	2.243(2)	2.265(4)
Co(1)–Cl(1)	2.269(1)	2.257(19)
Co(1)–Cl(2)	2.350(1)	2.3126(18)
Cl(1)–Co(1)–Cl(2)	114.91(4)	113.29(7)
Cl(2)–Co(1)–N(1)	90.50(7)	93.79(12)
Cl(2)–Co(1)–N(2)	99.76(7)	102.01(14)
Cl(2)–Co(1)–N(3)	88.06(7)	89.26(13)
N(1)–Co(1)–Cl(1)	98.82(7)	100.51(13)
N(1)–Co(1)–N(2)	80.45(8)	80.96(17)
N(1)–Co(1)–N(3)	160.08(7)	160.00(16)
N(2)–Co(1)–Cl(1)	145.33(6)	144.40(14)
N(2)–Co(1)–N(3)	80.23(8)	79.07(17)
N(3)–Co(1)–Cl(1)	99.79(7)	96.39(13)

In the IR spectrum the $\nu(\text{N–H})$ absorption bands are seen at *ca.* 3250 cm⁻¹ and shifted to a lower wavenumber than that in the corresponding free ligands. The magnetic susceptibility measurements for **3a** and **3b** reveal magnetic moments of *ca.* 3.95 μ_{B} (Evans balance at ambient temperature) which are indicative of high spin configurations possessing three unpaired electrons. The ¹H NMR spectra of **3a** and **3b** exhibit characteristic broad and paramagnetically shifted peaks but afforded no informative information with respect to peak assignment.

No DFT calculations were performed on the relative stability of the *mer*- and possible *fac*-isomers for **3**, but it is likely that the observed *mer* isomer is preferred on steric grounds. Similarly, a *mer* structure is observed in the related diamido complex [{(ArNCH₂CH₂)₂NMe}ZrMe₂] (Ar = 2,4,6-Me₃C₆H₂); formation of the alkyl cation notably leads to a facially coordinated species.¹

(c) Ethylene oligomerisation

All the complexes were tested for oligomerisation/polymerisation activity by treating them with 400 equivalents of MAO in toluene under an ethylene pressure (1 bar) and ambient temperature. In all cases oligomeric material was afforded; the results of the tests are shown in Table 6. The most active systems contain cobalt as the metal centre (**1** and **3**) with entry 1 the highest at 59 g mmol⁻¹ h⁻¹ bar⁻¹. The iron systems (entries 2 and 3) display much lower activities when compared to the corresponding cobalt complexes and are *ca.* 5000 times less active than most productive bis(imino)pyridine iron oligomerisation catalysts (under similar conditions).^{2,3}

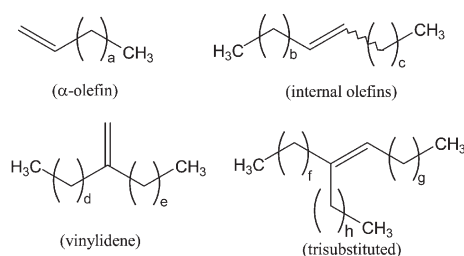
The nature of the oligomeric material does show some differences from that obtained using bis(imino)pyridine catalysts. While the iron-based systems behave similarly giving greater than 95% linear α -olefins (C₆–C₂₆), the cobalt systems give mixtures of linear and branched products (C₆–C₂₆). Indeed, extensive isomerisation is evident with terminal and internal olefins present along with vinylidenes, R¹R²C=CH₂, and small amounts of trisubstituted alkenes, R¹R²C=CHR³ (Fig. 8). For both the iron and cobalt systems a coordinative-insertion mechanism seems likely followed by a β -H elimination. To explain the branched components of the oligomers, insertion of a terminal olefin into a Co–R bond seems likely, followed by β -H elimination. For both the iron systems the oligomeric distribution is found to follow a Schulz–Flory distribution for both **2a** and **2b** with the Schulz–Flory parameter α in both cases being around 0.8.¹⁵

The observation that **1** and **2** result in oligomeric materials is consistent with a rapid chain transfer process as a consequence of there being insufficient steric bulk to prevent associative displacement of the growing oligomeric chain. Indeed iron complexes containing sterically bulky 2-iminopyridine ligands afford only short-chain oligomeric products.¹⁶ However, for **3** which possess 2,6-substituted groups on both sides of the

Table 6 Ethylene oligomerisation with the iron(II) and cobalt(II) catalysts

Entry ^a	Pre-catalyst	Yield ^b (%)	Activity/g mmol ⁻¹ h ⁻¹ bar ⁻¹	Internal olefin ^c (%)	External olefin ^c (%)	Branched ^c (%)	Av. chain length, ^c C _n
1	1a	0.295	59	63.6	25.5	10.9	12.7
2	1b	0.131	26	59.7	29.9	10.4	11.7
3	2a	0.020	4	1.0	98.5	0.5	6.5
4	2b	0.025	5	0.7	99.3	—	6.87
5	3a	0.206	41	61.5	27.3	11.2	11.3
6	3b	0.198	40	62.2	27.7	10.1	10.6

^a General conditions: 1 bar ethylene Schlenk test carried out in toluene (40 cm³) at ambient temperature, using 4.0 mmol MAO (Al:M = 400:1), 0.01 mmol precatalyst, over 30 min. Reactions terminated by addition of dilute HCl. ^b Yield calculated based on GC using a C₁₇ internal standard. ^c Oligomerisation product percentages and average chain length, C_n calculated *via* integration of ¹H NMR spectra.

**Fig. 8** Types of oligomeric product obtained using cobalt catalysts (**1a**, **1b**, **3a** and **3b**).

molecule it might be expected that polymeric material would result; the explanation for this observation is unclear.

(d) Conclusions

A series of iron and cobalt chloride complexes (**1**, **2**) containing aryl-substituted *N*-picolylen ligands have been prepared and fully characterised. Both the experimental results and calculations indicate that *fac*- and *mer*-structures are possible for this ligand type with the energy difference between each minimal. Moreover, interconversion between structures in solution has been shown to be a facile process. Application of **1** and **2** along with the aryl-substituted dien cobalt complexes (**3**) as catalysts for the oligomerisation of ethylene has been demonstrated. While only modest activities result, both linear and branched oligomeric materials are accessible. The conformation of the tridentate nitrogen donor ligands in the catalytically active species is uncertain and will be the subject of further studies.

3 Experimental

3.1 General

All reactions were carried out under an atmosphere of dry, oxygen-free nitrogen, using standard Schlenk techniques or in a nitrogen purged glove box. Solvents were distilled under nitrogen from appropriate drying agents and degassed prior to use.¹⁷ The infrared spectra were recorded as Nujol mulls between 0.5 mm NaCl plates on a Perkin Elmer 1600 series or in the solid state using a Perkin Elmer Spectrun One FT-IR spectrometer. The ES and the FAB mass spectra were recorded using a micromass Quattro LC mass spectrometer and a Kratos Concept spectrometer with methanol or NBA as the matrix respectively. ¹H and ¹³C NMR spectra were recorded on a Bruker ARX spectrometer 250 or 300 MHz; chemical shifts (ppm) are referred to the residual protic solvent peaks; relaxation times (τ₁) are in milliseconds. GC mass spectrometry measurements were obtained using a Perkin Elmer Autosystem XL chromatogram and a Perkin Elmer Turbo Mass Spectrometer. Magnetic susceptibility studies were performed using an Evans Balance (Johnson Matthey) at room temperature. The magnetic moment was calculated following standard methods¹⁸ and corrections for underlying diamagnetism were applied to data.¹⁹ Elemental analyses were performed at the Department of Chemistry, University of North London by Dr S. Boyer.

The reagents, 2-(aminomethyl)pyridine, diethylenetriamine, sodium *tert*-butoxide, the aryl halides, MAO (10% wt solution in toluene) and the metal dichlorides were purchased from Aldrich Chemical Co. and used without further purification. *rac*-BINAP was purchased from Strem Chemical Co. Ethylene gas (Grade 3.5) was supplied from BOC. The compounds, Pd₂(dba)₃,²⁰ and {(2,4,6-Me₃C₆H₂)NHCH₂CH₂}₂NH^{1b} were prepared according to previously reported procedures. All other chemicals were obtained commercially and used without further purification.

3.2 Synthesis of (H₂NCH₂CH₂){(2-C₅H₄N)CH₂}NH

The preparation was carried out based on a modification of the literature report.²¹ 2-Chloroethylamine monohydrochloride (12.0 g, 0.103 mol) was added in portions to an ice-cooled solution of sodium hydroxide (51.5 cm³, 2 M NaOH, 0.103 mol). This was repeated and the contents of the two flasks (0.206 mol) combined. The free 2-chloroethylamine was then added dropwise to a rapidly stirred solution of 2-(aminomethyl)pyridine (44.0 g, 0.407 mol) in absolute ethanol (50 cm³) and refluxed for 2 h. The volatiles were removed by rotary evaporation, the residue poured onto crushed ice and excess KOH pellets added. The dark orange-brown solution was extracted with CHCl₃ (3 × 100 cm³). The combined extracts were dried over MgSO₄, filtered and taken to dryness to give an oily residue. Distillation of the residue under reduced pressure (3.0 × 10⁻¹ mmHg) gave unreacted 2-(aminomethyl)pyridine (44 °C) as the first fraction followed by (H₂NCH₂CH₂){(2-C₅H₄N)CH₂}NH (9.1 g, 26%) (84 °C) as a pale yellow liquid. FAB mass spectrum, *m/z* 151 (M⁺). NMR (CDCl₃, 293 K): ¹H, δ 8.7–7.0 (m, 4H, Py-H), 3.9 (s, 2H, PyCH₂, 2H), 2.87 (m, 2H, CH₂), 2.78 (s, 2H, CH₂) and 1.6 (s, br, 3H, NH). ¹³C (1H composite pulse decoupled), δ 159.8 (s, C, Py), 149.0 (s, C, Py), 136.2 (s, C, Py), 122.2 (s, C, Py), 121.9 (s, C, Py), 55.2 (s, CH₂), 50.8 (s, CH₂) and 41.7 (s, CH₂).

3.3 Synthesis of (ArNHCH₂CH₂){(2-C₅H₄N)CH₂}NH

(i) (Ar = 2,6-Me₂C₆H₃). A Schlenk flask was charged with (H₂NCH₂CH₂){(2-C₅H₄N)CH₂}NH (1.00 g, 6.62 mmol), 2-bromo-*m*-xylene (0.88 cm³, 1.23 g, 6.62 mmol), Pd₂(dba)₃ (0.030 g, 0.033 mmol, 0.005 equiv.), *rac*-BINAP (0.062 g, 0.099 mmol, 0.015 equiv.), NaOBu^t (1.91 g, 19.9 mmol, 3 equiv.) and toluene (40 cm³). The reaction mixture was heated to 100 °C and stirred for a period of 4 days. After cooling to room temperature, the solvent was removed under reduced pressure to afford an oily residue. The residue was dissolved in diethyl ether (30 cm³) and washed with water (3 × 30 cm³) and saturated sodium chloride solution (3 × 30 cm³). The organic layer was separated and dried over magnesium sulfate. The volatiles were removed under reduced pressure and the residue left under vacuum at 70 °C for 24 h to give 1.30 g (77%) of {(2,6-Me₂C₆H₃)HNCH₂CH₂}{(2-C₅H₄N)CH₂}NH as a viscous oil. ES mass spectrum, *m/z* 256 (M⁺ + H). NMR (CDCl₃, 293 K): ¹H, δ 8.5–7.0 (m, 4H, Py-H), 6.88 (m, 2H, Ar-H), 6.70 (m, 1H, Ar-H), 3.85 (s, 2H, PyCH₂, 2H), 3.02 (t, 2H, ³J(HH) 5.7, CH₂),

2.77 (t, 2H, CH₂) and 2.20 (s, 6H, Me_o). ¹³C (¹H composite pulse decoupled), δ 160.3 (s, C, Py), 149.7 (s, C, Py), 146.8 (s, C, Ar), 136.9 (s, C, Py), 129.7 (s, C, Ar), 129.2 (s, C, Ar), 122.6 (s, C, Py), 122.4 (s, C, Py), 121.9 (s, C, Ar), 55.4 (s, CH₂), 50.0 (s, CH₂), 48.4 (s, CH₂) and 19.0 (s, Me_o).

(ii) (Ar = 2,4,6-Me₃C₆H₂). Using the same procedure and molar quantities of reagents as above in 3.3(i) but with 2-bromomesitylene (1.00 cm³, 1.32 g, 6.62 mmol) as the aryl bromide, {(2,4,6-Me₃C₆H₂)HNCH₂CH₂}₂{(2-C₅H₄N)CH₂}NH (1.43 g, 80%) was isolated as a red oil. ES mass spectrum, *m/z* 270 (M⁺ + H). NMR (CDCl₃, 293 K): ¹H, δ 8.5–7.1 (m, 4H, Py-H), 6.72 (s, 2H, Ar-H), 3.86 (s, 2H, PyCH₂), 2.98 (t, 2H, ³J(HH) 6.0, CH₂), 2.89 (t, 2H, CH₂), 2.29 (s, 6H, Me_o) and 2.21 (s, 3H, Me_p). ¹³C (¹H composite pulse decoupled), δ 160.3 (s, C, Py), 149.7 (s, C, Py), 144.1 (s, C, Ar), 136.7 (s, C, Py), 131.4 (s, C, Py), 130.0 (s, C, Ar), 129.4 (s, C, Ar), 122.6 (s, C, Py), 122.4 (s, C, Ar), 55.5 (s, CH₂), 50.0 (s, CH₂), 48.7 (s, CH₂), 20.9 (s, Me_p) and 18.8 (s, Me_o).

3.4 Synthesis of {(2,6-Me₂C₆H₃)HNCH₂CH₂}₂NH

A Schlenk flask was charged with (H₂NCH₂CH₂)₂NH (1.06 g, 10.3 mmol), 2-bromo-*m*-xylene (2.74 cm³, 3.81 g, 20.6 mmol), Pd₂(dba)₃ (0.047 g, 0.052 mmol, 0.005 equiv.), *rac*-BINAP (0.096 g, 0.155 mmol, 0.015 equiv.), NaOBu^t (2.97 g, 30.9 mmol) and toluene (40 cm³). The reaction mixture was heated to 100 °C and stirred for a period of 4 days. After cooling to room temperature, the solvent was removed under reduced pressure to afford an oily residue. The residue was dissolved in diethyl ether (30 cm³) and washed with water (3 × 30 cm³) and saturated sodium chloride solution (3 × 30 cm³). The organic layer was separated and dried over magnesium sulfate. The solvent was removed under reduced pressure and the residue left under vacuum at 70 °C for 24 h to give 2.46 g (77%) of {(2,6-Me₂C₆H₃)HNCH₂CH₂}₂NH as a viscous oil. ES mass spectrum, *m/z* 312 (M⁺ + H). IR (cm⁻¹): 3358 (NH, medium). NMR (CDCl₃, 293 K): ¹H NMR (CDCl₃): δ 6.89 (d, 4H, ³J(HH) 7.3, Ar-H_m), 6.72 (t, 2H, Ar-H_p), 3.00 (t, 4H, ³J(HH) 6.0, CH₂), 2.76 (t, 4H, CH₂) and 2.22 (s, 12H, Me_o). ¹³C (¹H composite pulse decoupled), δ 146.4 (s, C, Ar), 129.4 (s, C, Ar), 128.9 (s, C, Ar), 121.8 (s, C, Ar), 50.1 (s, CH₂), 48.3 (s, CH₂) and 18.7 (s, Me_o).

3.5 Synthesis of [(ArNHCH₂CH₂)₂(2-C₅H₄N)CH₂]-NH₂CoCl₂] (1)

(i) (Ar = 2,6-Me₂C₆H₃). A solution of {(2,6-Me₂C₆H₃)HNCH₂CH₂}₂{(2-C₅H₄N)CH₂}NH (0.100 g, 0.39 mmol) in *n*-butanol was introduced dropwise to a solution of CoCl₂ (0.051 g, 0.39 mmol) in *n*-butanol (5 cm³) at 90 °C to form a green solution. After being stirred at 90 °C for 1 h, the reaction was allowed to cool to room temperature. The reaction mixture was concentrated and hexane added to induce precipitation of the product as a pale blue solid. The suspension was stirred overnight, filtered, washed with hexane (2 × 30 cm³) and dried under reduced pressure to afford 0.121 g (80%) of **1a** as a pale blue powder. Layering of an acetonitrile solution of **1a** with hexane gave blue crystals of **1a** on prolonged standing. ¹H NMR (acetonitrile-*d*₃): δ 113.8 (4.1 ms, H_a), 110.1 (1.0 ms, NH), 97.0 (0.8 ms, CH₂), 87.3 (1.1 ms, CH₂), 45.7 (15.9 ms, H_β), 42.5 (25.9 ms, H_β), 13.5 (2.9 ms, CH₂), 11.8 (43.2 ms, Ar-CH_m), -3.6 (poor data set, 52.8 ms, H_γ), -9.1 (Ar-CH_p), -14.1 (poor data set, 5.3 ms, ArMe_o), -40.0 (NH).

(ii) (Ar = 2,4,6-Me₃C₆H₂). Using the same procedure and molar quantities of reagents as above in 3.5(i) using {(2,4,6-Me₃C₆H₂)HNCH₂CH₂}₂{(2-C₅H₄N)CH₂}NH and CoCl₂, gave 0.117 g (75%) of **1b** as a pale blue powder. Layering of an acetonitrile solution of **1b** with hexane gave blue crystals on prolonged standing. ¹H NMR (acetonitrile-*d*₃): δ 116.7 (9.3 ms, H_a), 104.6 (1.5 ms, NH), 90.1 (0.8 ms, CH₂), 86.9 (0.9 ms, CH₂), 46.6 (15.0 ms, H_β), 44.0 (23.2 ms, H_β), 16.4 (poor data set, 135.4 ms,

ArMe_p), 12.5 (45.3 ms, Ar-CH_m), -3.0 (52.6 ms, H_γ), -11.8 (2.2 ms, ArMe_o).

3.6 Synthesis of [(ArNHCH₂CH₂)₂(2-C₅H₄N)CH₂]-NH₂FeCl₂] (2)

(i) (*n* = 1, Ar = 2,6-Me₂C₆H₃). A solution of {(2,6-Me₂C₆H₃)HNCH₂CH₂}₂{(2-C₅H₄N)CH₂}NH (0.100 g, 0.39 mmol) in *n*-butanol was introduced dropwise to a solution of FeCl₂ (0.050 g, 0.39 mmol) in *n*-butanol (5 cm³) at 90 °C to form a yellowish green solution. After being stirred at 90 °C for 1 h, the reaction was allowed to cool to room temperature. The reaction mixture was concentrated and hexane added to induce precipitation of the product as a yellow solid. The suspension was stirred overnight, filtered, washed with hexane (2 × 30 cm³) and dried under reduced pressure to afford 0.115 g (77%) of **2a** as a yellow–brown powder. Layering of an acetonitrile solution of **2a** with hexane gave golden crystals on prolonged standing. ¹H NMR (acetonitrile-*d*₃, 293 K): δ 130.4 (poor data set, 65.6 ms, H_a), 124.1 (3.8 ms, NH), 104.9 (0.96 ms, CH₂), 80.9 (0.73 ms, CH₂), 62.9 (0.9 ms, CH₂), 58.8 (16.4 ms, H_β), 57.4 (14.6 ms, H_β), 15.8 (37.1 ms, H_γ), 12.3 (34.2 ms, Ar-CH_m), 6.6 (2.0 ms, ArMe_o), -5.4 (poor data set, 143 ms, Ar-CH_p), -15.0 (15.3 ms, NH).

(ii) (*n* = 2, Ar = 2,4,6-Me₃C₆H₂). Using the same procedure and molar quantities of reagents as above in 3.6(i) using {(2,4,6-Me₃C₆H₂)HNCH₂CH₂}₂{(2-C₅H₄N)CH₂}NH and FeCl₂, gave 0.107 g (80%) of **2b** as a yellow–brown powder. Layering of an acetonitrile solution of **2b** with hexane gave golden crystals on prolonged standing. ¹H NMR (acetonitrile-*d*₃, 293 K): δ 129.6 (0.9 ms, H_a), 120.0 (1.9 ms, NH), 108.1 (1.7 ms, CH₂), 82.4 (1.1 ms, CH₂), 63.9 (0.7 ms, CH₂), 58.6 (13.2 ms, H_β), 56.6 (11.2 ms, H_β), 16.8 (90.3 ms, H_γ), 15.7 (29.1 ms, ArMe_p), 11.6 (27.8 ms, Ar-CH_m), 7.4 (2.5 ms, ArMe_o), -12.7 (4.0 ms, NH).

3.7 Synthesis of [(ArNHCH₂CH₂)₂NH]CoCl₂] (3)

(i) Ar = 2,6-Me₂C₆H₃. A solution of {(2,6-Me₂C₆H₃)HNCH₂CH₂}₂NH (0.100 g, 0.32 mmol) in *n*-butanol was added dropwise to a solution of CoCl₂ (0.042 g, 0.32 mmol) in *n*-butanol (5 cm³) at 90 °C to yield a green solution. After being stirred at 90 °C for 1 h, the reaction was allowed to cool to room temperature. The reaction mixture was concentrated and hexane added to induce precipitation of the product as a pale blue solid. The suspension was stirred overnight, filtered, washed with hexane (2 × 30 cm³) and dried under reduced pressure to afford 0.121 g (80%) of **3a** as a pale blue solid. Layering of an acetonitrile solution of **3a** with hexane gave pale blue crystals of on prolonged standing.

(ii) Ar = 2,4,6-Me₃C₆H₂. Using the same procedure and molar quantities of reagents as above in 3.7(i) using {(2,4,6-Me₃C₆H₂)HNCH₂CH₂}₂NH and CoCl₂, gave 0.112 g (75%) of **3b** as a pale blue powder. Layering of an acetonitrile solution of **3b** with hexane gave pale blue crystals of on prolonged standing.

3.8 Ethylene oligomerisation

The precatalyst (**1–3**) (0.01 mmol) was added to a Schlenk tube, dissolved or suspended in toluene (40 ml) and MAO (4.0 mmol, 400 equiv.) introduced. The tube was purged with ethylene and the contents stirred under 1 bar ethylene at room temperature for the duration of the test. After 0.5 h the test was terminated by the addition of dilute aqueous hydrogen chloride. The organic phase was separated, analysed by GC and then the solvent removed by distillation and the residue analysed by NMR spectroscopy.

3.9 Density functional calculations

Quantum mechanical calculations have been carried out using the Gaussian 98 package of programs.²² The density functional theory (DFT) was applied, in particular the functional Becke's

Table 7 Crystallographic and data processing parameters for complexes **1a**, **1b**, **2a**, **2b**, **3a** and **3b**

Complex	1a	1b	2a	2b	3a	3b
Formula	C ₁₆ H ₂₁ Cl ₂ CoN ₃	C ₁₇ H ₂₃ Cl ₂ CoN ₃ ·MeCN	C ₁₆ H ₂₁ Cl ₂ FeN ₃	C ₁₇ H ₂₃ Cl ₂ FeN ₃	C ₂₀ H ₂₉ Cl ₂ CoN ₃	C ₂₃ H ₃₃ Cl ₂ CoN ₃
<i>M</i>	385.19	440.27	382.11	396.13	441.29	469.34
Crystal size/mm	0.28 × 0.24 × 0.21	0.24 × 0.15 × 0.07	0.66 × 0.32 × 0.28	0.34 × 0.11 × 0.04	0.56 × 0.32 × 0.14	0.52 × 0.12 × 0.09
<i>T</i> /K	150(2)	150(2)	120(2)	150(2)	200(2)	200(2)
Crystal system	Monoclinic	Triclinic	Orthorhombic	Monoclinic	Triclinic	Monoclinic
Space group	<i>P</i> 2 ₁ / <i>c</i>	<i>P</i> 1̄	<i>P</i> bca	<i>C</i> 2/ <i>c</i>	<i>P</i> 1̄	<i>P</i> 2 ₁ / <i>c</i>
Lattice parameters						
<i>a</i> /Å	14.5732(7)	8.6478(8)	16.1151(2)	28.7059(19)	6.484(3)	13.143(5)
<i>b</i> /Å	7.5761(4)	10.6957(10)	12.9294(1)	9.5482(6)	10.962(6)	15.618(6)
<i>c</i> /Å	16.3162(8)	11.9131(11)	16.3990(2)	14.2018(10)	15.778(5)	11.783(8)
<i>a</i> /°	90	82.715(2)	90	90	103.21(5)	90
<i>β</i> /°	108.481(15)	68.821(2)	90	112.226(1)	96.16(4)	102.07(5)
<i>γ</i> /°	90	85.749(2)	90	90	100.35(3)	90
<i>V</i> /Å ³	1708.5(2)	1018.7(2)	3424.59(7)	3603.3(4)	1061.1(8)	2365(2)
<i>Z</i>	4	2	8	8	2	4
<i>D</i> _c /Mg m ⁻³	1.497	1.435	1.482	1.460	1.381	1.318
<i>F</i> (000)	796	458	1584	1648	462	988
<i>μ</i> (Mo-Kα)/mm ⁻¹	1.316	1.115	1.192	1.136	1.069	0.964
Reflections collected	13898	8606	21314	12725	4388	4674
Independent reflections	3716	4357	3013	3170	3859	4083
<i>R</i> _{int}	0.021	0.034	0.0473	0.039	0.025	0.0480
Parameters/restraints	201/0	239/0	201/0	211/0	235/0	253/0
Final <i>R</i> indices						
<i>I</i> > 2σ(<i>I</i>)	<i>R</i> ₁ = 0.026 <i>wR</i> ₂ = 0.068	<i>R</i> ₁ = 0.033 <i>wR</i> ₂ = 0.065	<i>R</i> ₁ = 0.0255 <i>wR</i> ₂ = 0.0689	<i>R</i> ₁ = 0.033 <i>wR</i> ₂ = 0.071	<i>R</i> ₁ = 0.033 <i>wR</i> ₂ = 0.077	<i>R</i> ₁ = 0.0610 <i>wR</i> ₂ = 0.1165
All data	<i>R</i> ₁ = 0.029 <i>wR</i> ₂ = 0.069	<i>R</i> ₁ = 0.048 <i>wR</i> ₂ = 0.067	<i>R</i> ₁ = 0.0281 <i>wR</i> ₂ = 0.0701	<i>R</i> ₁ = 0.043 <i>wR</i> ₂ = 0.074	<i>R</i> ₁ = 0.042 <i>wR</i> ₂ = 0.082	<i>R</i> ₁ = 0.1312 <i>wR</i> ₂ = 0.1405
Goodness of fit on <i>F</i> ² (all data)	1.039	0.862	1.146	0.990	1.061	0.966

Data in common: graphite-monochromated Mo-Kα radiation, λ = 0.71073 Å; *R*₁ = Σ|*F*_o - |*F*_c||Σ|*F*_o|, *wR*₂ = [Σ*w*(*F*_o² - *F*_c²)²/Σ*w*(*F*_o²)]^{1/2}, *w*⁻¹ = [σ²(*F*_o)² + (*aP*)²], *P* = [(max(*F*_o², 0) + 2(*F*_c²))/3], where *a* is a constant adjusted by the program; goodness of fit = [Σ(*F*_o² - *F*_c²)²/(*n* - *p*)]^{1/2}, where *n* is the number of reflections and *p* the number of parameters.

three-parameter hybrid exchange method combined with LYP correlation functional (B3LYP).²³ The method was used in its unrestricted implementation.

The quasi-relativistic effective core potential (ECP) LANL2DZ was used for the metal atoms (Co and Fe).²⁴ The basis set for both atoms is the valence double- ζ contraction associated to this ECP.^{22,24} The valence double- ζ with polarisation 6–31G(d)^{25,26} basis was used for N and Cl and the valence double- ζ 6–31G for C and H.²⁵ In all cases, the spin contamination, evaluated from the computed value of S^2 , was found to be small.

3.10 Crystallography

Data for **1a**, **1b**, **2a** and **2b** were collected on a Bruker APEX 2000 CCD diffractometer, data for **3a** and **3b** were collected on a Bruker P4 diffractometer. Details of data collection, refinement and crystal data are listed in Table 7. The data were corrected for Lorentz and polarisation effects and empirical absorption corrections applied. Structure solution by Patterson methods and structure refinement on F^2 employed SHELXTL version 6.10.^{27,28} Hydrogen atoms were included in calculated positions (C–H = 0.96 Å) riding on the bonded atom with isotropic displacement parameters set to $1.5U_{eq}(C)$ for methyl H atoms and $1.2U_{eq}(C)$ for all other H atoms. All non H atoms were refined with anisotropic displacement parameters.

CCDC reference numbers 243370–243375.

See <http://www.rsc.org/suppdata/dt/b4/b409827g/forcrystallographic> data in CIF or other electronic format.

Acknowledgements

We thank the EPSRC (to C. J. D.), ExxonMobil (to C. J. D.) and the Nuffield Foundation for an Undergraduate Summer Bursary (to S. J. H.) for financial assistance. Financial and equipment support from the Department of Chemistry at the University of Leicester and the Royal Society are gratefully acknowledged. Johnson Matthey PLC are thanked for their loan of palladium chloride. Finally, Dr Feliu Maseras (ICIQ) and Professor Michael Sutcliffe (Leicester) are sincerely acknowledged for their valuable advice.

References

- (a) R. R. Schrock, A. L. Casado, J. T. Goodman, L.-C. Liang, P. J. Bonitatebus, Jr. and W. M. Davis, *Organometallics*, 2000, **19**, 5325; (b) L.-C. Liang, R. R. Schrock, W. M. Davis and D. H. McConville, *J. Am. Chem. Soc.*, 1999, **121**, 5797; (c) R. R. Schrock, P. J. Bonitatebus, Jr. and Y. Schrodi, *Organometallics*, 2001, **20**, 1056; (d) Y. Schrodi, R. R. Schrock and P. J. Bonitatebus, Jr., *Organometallics*, 2001, **20**, 3560.
- (a) B. L. Small and M. Brookhart, *J. Am. Chem. Soc.*, 1998, **120**, 7143; (b) B. L. Small, M. Brookhart and A. M. A. Bennett, *J. Am. Chem. Soc.*, 1998, **120**, 4049; (c) A. M. A. Bennett, *Int. Pat.*, WO 98/27124, 1998 (Dupont); A. M. A. Bennett, *Chem. Abstr.*, 1998, **129**, 122973x.
- (a) G. J. P. Britovsek, V. C. Gibson, B. S. Kimberley, P. J. Maddox, S. J. McTavish, G. A. Solan, A. J. P. White and D. J. Williams, *Chem. Commun.*, 1998, 849; (b) G. J. P. Britovsek, M. Bruce, V. C. Gibson, B. S. Kimberley, P. J. Maddox, S. Mastroianni, S. J. McTavish, C. Redshaw, G. A. Solan, S. Strömberg, A. J. P. White and D. J. Williams, *J. Am. Chem. Soc.*, 1999, **121**, 8728; (c) G. J. P. Britovsek, B. A. Dorer, V. C. Gibson, B. S. Kimberley and G. A. Solan, *Int. Pat.*, WO 99/12981, 1999 (BP Chemicals Ltd); G. J. P. Britovsek, B. A. Dorer, V. C. Gibson, B. S. Kimberley and G. A. Solan, *Chem. Abstr.*, 1999, **130**, 252793.
- D. Reardon, F. Conan, S. Gambarotta, G. Yap and Q. Wang, *J. Am. Chem. Soc.*, 1999, **121**, 9318.
- C. J. Davies, J. Fawcett and G. A. Solan, *Polyhedron*, 2004, submitted.
- (a) J. P. Wolfe, S. Wagsaw and S. L. Buchwald, *J. Am. Chem. Soc.*, 1996, **118**, 7215; (b) F. Paul, J. Patt and J. F. Hartwig, *J. Am. Chem. Soc.*, 1994, **116**, 5969.
- Cl–Co–Cl range (for [bis(imino)pyridine]CoCl₂ complexes): 112.9–120.1°; (a) see refs. 2a and 3b; (b) T. M. Kooistra, K. F. W. Hekking, Q. Knijnenburg, B. de Bruin, P. H. M. Budzelaar, R. de Gelder, J. M. M. Smits and A. W. Gal, *Eur. J. Inorg. Chem.*, 2003, 648; (c) Y. Chen, C. Qian and J. Sun, *Organometallics*, 2003, **22**, 1231; (d) C. Bianchini, G. Mantovani, A. Meli, F. Migliacci, F. Zanobini, F. Laschi and A. Sommacchi, *Eur. J. Inorg. Chem.*, 2003, 1620.
- Cl–Co–Cl range (general): 101.8–134.4°; (a) see ref. 7b; (b) N. di Vaira and P. L. Orioli, *Inorg. Chem.*, 1969, **8**, 2729; (c) Z. Dori, R. Eisenberg and H. B. Gray, *Inorg. Chem.*, 1967, **6**, 483; (d) M. Gerloch, *J. Chem. Soc. A*, 1966, 1317; (e) S. J. Shieh, C.-C. Chou, G.-H. Lee, C.-C. Wang and S.-M. Peng, *Angew. Chem., Int. Ed. Engl.*, 1997, **36**, 56; (f) S.-C. Sheu, M.-J. Tien, M.-C. Cheng, T.-I. Ho, S. M. Peng and Y.-C. Lin, *J. Chem. Soc., Dalton Trans.*, 1995, 3503.
- Cl–Fe–Cl range (for [bis(imino)pyridine]FeCl₂ complexes): 106.9–118.3°; (a) see refs. 2, 3 and 7c; (b) Y. Chen, R. Chen, C. Qian, Y. Dang and J. Sun, *Organometallics*, 2003, **22**, 4312.
- (a) M. Ito, Y. Takita, K. Sakai and T. Tubomura, *Chem. Lett.*, 1998, 1185; (b) E. S. Raper, A. Miller, T. Glowiak and M. Kubiak, *Transition Met. Chem.*, 1989, **14**, 319; (c) D. A. Handley, P. B. Hitchcock, T.-H. Lee and G. J. Leigh, *Inorg. Chim. Acta*, 2001, **314**, 14; (d) S. Kasselouri, A. Garoufis, S. P. Perlepes, F. Lutz, R. Bau, S. Gourbatsis and N. Hadjiliadis, *Polyhedron*, 1998, **17**, 1281; (e) V. C. Gibson, R. K. O'Reilly, D. F. Wass, A. J. P. White and D. J. Williams, *Dalton Trans.*, 2003, 2824.
- C. J. Davies, A. Harrison and G. A. Solan, unpublished results.
- D. Mandon, A. Machkour, S. Goetz and R. Welter, *Inorg. Chem.*, 2002, **41**, 5364.
- H. C. S. Clark, F. G. N. Cloke, P. B. Hitchcock, J. B. Love and A. P. Wainwright, *J. Organomet. Chem.*, 1995, **501**, 333.
- J. D. Maréchal, G. Barea, F. Maseras, A. Llenos, L. Mouawad and D. Perahia, *J. Comput. Chem.*, 1999, **21**, 283.
- (a) P. J. Flory, *J. Am. Chem. Soc.*, 1940, **62**, 1561; (b) G. V. Schulz, *Z. Phys. Chem., B*, 1935, **30**, 379; (c) G. V. Schulz, *Z. Phys. Chem., B*, 1939, **43**, 25.
- G. J. P. Britovsek, S. P. D. Baugh, O. Hoarau, V. C. Gibson, D. F. Wass, A. J. P. White and D. J. Williams, *Inorg. Chim. Acta*, 2003, **345**, 279.
- W. L. F. Armarego and D. D. Perrin, *Purification of Laboratory Chemicals*, Butterworth–Heinemann, 4th edn., 1996.
- F. E. Mabbs and D. J. Machin, *Magnetism and Transition Metal Complexes*, Chapman and Hall, London, 1973.
- C. J. O'Connor, *Prog. Inorg. Chem.*, 1982, **29**, 203; *Handbook of Chemistry and Physics*, ed. R. C. Weast, CRC Press, Boca Raton, FL, 70th edn., 1990, p. E134.
- T. Ukai, H. Kawazura, Y. Ishii, J. J. Bonnett and J. A. Ibers, *J. Organomet. Chem.*, 1974, **65**, 253.
- G. Riggio, W. H. Hopff, A. A. Hofmann and P. G. Waser, *Helv. Chim. Acta.*, 1980, **63**, 488.
- Gaussian 98* (Revision A.11.4), M. J. Frisch, G. W. Trucks, H. B. Schlegel, G. E. Scuseria, M. A. Robb, J. R. Cheeseman, V. G. Zakrzewski, J. A. Montgomery, Jr., R. E. Stratmann, J. C. Burant, S. Dapprich, J. M. Millam, A. D. Daniels, K. N. Kudin, M. C. Strain, O. Farkas, J. Tomasi, V. Barone, M. Cossi, R. Cammi, B. Mennucci, C. Pomelli, C. Adamo, S. Clifford, J. Ochterski, G. A. Petersson, P. Y. Ayala, Q. Cui, K. Morokuma, P. Salvador, J. J. Dannenberg, D. K. Malick, A. D. Rabuck, K. Raghavachari, J. B. Foresman, J. Cioslowski, J. V. Ortiz, A. G. Baboul, B. B. Stefanov, G. Liu, A. Liashenko, P. Piskorz, I. Komaromi, R. Gomperts, R. L. Martin, D. J. Fox, T. Keith, M. A. Al-Laham, C. Y. Peng, A. Nanayakkara, M. Challacombe, P. M. W. Gill, B. Johnson, W. Chen, M. W. Wong, J. L. Andres, C. Gonzalez, M. Head-Gordon, E. S. Replogle and J. A. Pople, Gaussian, Inc., Pittsburgh PA, 2001.
- (a) A. D. Becke, *J. Chem. Phys.*, 1993, **98**, 5648; (b) C. Lee, W. Yang and R. G. Parr, *Phys. Rev. B: Condens. Matter*, 1988, **37**, 785; (c) P. J. Stephens, F. J. Devlin, C. F. Chabalowski and M. J. Frisch, *J. Phys. Chem.*, 1994, **98**, 11623.
- P. J. Hay and W. R. Wadt, *J. Chem. Phys.*, 1985, **82**, 299.
- W. J. Hehre, R. Ditchfield and J. A. Pople, *J. Chem. Phys.*, 1972, **56**, 2257.
- P. C. Hariharan and J. A. Pople, *Theor. Chim. Acta.*, 1973, **28**, 213.
- G. M. Sheldrick, *SHELXS97, program for crystal structure solution*, University of Göttingen, Germany, 1993.
- G. M. Sheldrick, *SHELXL97, program for crystal structure refinement*, University of Göttingen, Germany, 1993.